A Novel Strategy for Quantifying Choriocapillaris Flow Voids Using Swept-Source OCT Angiography

Qinqin Zhang,[1] Fang Zheng,[2] Elie H. Motulsky,[2] Giovanni Gregori,[2] Zhongdi Chu,[1] Chieh-Li Chen,[1] Chunxia Li,[1] Luis de Sisternes,[3] Mary Durbin,[3] Philip J. Rosenfeld,[2] and Ruikang K. Wang[1,4]

[1]Department of Bioengineering, University of Washington, Seattle, Washington, United States
[2]Department of Ophthalmology, Bascom Palmer Eye Institute, University of Miami Miller School of Medicine, Miami, Florida, United States
[3]Advanced Development, Carl Zeiss Meditec, Inc., Dublin, California, United States
[4]Department of Ophthalmology, University of Washington Eye Institute, Seattle, Washington, United States

Correspondence: Ruikang K. Wang, Department of Bioengineering, University of Washington, Seattle, WA 98195, USA;
wangrk@uw.edu.

Submitted: September 11, 2017
Accepted: November 16, 2017

Citation: Zhang Q, Zheng F, Motulsky EH, et al. A novel strategy for quantifying choriocapillaris flow voids using swept-source OCT angiography. *Invest Ophthalmol Vis Sci*. 2018;59:203–211. https://doi.org/10.1167/iovs.17-22953

Purpose. To achieve reproducible imaging of the choriocapillaris and associated flow voids using swept-source OCT angiography (SS-OCTA).

Methods. Subjects were enrolled and SS-OCTA was performed using the 3 × 3 mm scan pattern. Blood flow was identified using the complex optical microangiography (OMAG) algorithm. The choriocapillaris was defined as a slab from the outer boundary of Bruch's membrane (BM) to approximately 20 μm below BM. Compensation for the shadowing effect caused by the RPE and BM complex on the choriocapillaris angiogram was achieved by using the structural information from the same slab. A thresholding method to calculate the percentage of flow voids from a region was developed based on a normal database.

Results. Twenty normal subjects and 12 subjects with drusen were enrolled. SS-OCTA identified the choriocapillaris in normal subjects as a lobular plexus of capillaries in the central macula and the lobular arrangement became more evident toward the periphery. In all eyes, signal compensation resulted in fewer choriocapillaris flow voids with improved repeatability of measurements. The best repeatability for the measurement was achieved by using 1 standard deviation (SD) for the thresholding strategy.

Conclusions. SS-OCTA can image the choriocapillaris in vivo, and the repeatability of flow void measurements is high in the presence of drusen. The ability to image the choriocapillaris and associated flow voids should prove useful in understanding disease onset, progression, and response to therapies.

Keywords: optical coherence tomography angiography, OCTA, swept-source OCTA, choriocapillaris, flow voids

The choriocapillaris is a single-layer capillary meshwork located at the inner boundary of the choroid, which is adjacent to Bruch's membrane (BM) and the retinal pigment epithelium (RPE).[1] This thin, dense capillary network has a lobular pattern, and in normal eyes, has a thickness of approximately 10 μm. This capillary network provides nourishment and metabolic exchange to the RPE and outer retina through fenestrations on its inner surface. Loss of the choriocapillaris would deprive the RPE and outer retina of oxygen and needed nutrients resulting in an abnormal, ischemic environment.

In 1999, Lutty et al.[2] found that the choriocapillaris blood flow in the fovea decreased with age and decreased further in subjects with age-related macular degeneration (AMD). In donor eyes with late AMD, geography atrophy (GA) was accompanied by the loss of the photoreceptors, RPE, choriocapillaris, and inner choroid.[3] McLeod et al.[4] reported similar findings in eyes with late nonexudative AMD and GA, and they also showed a linear relationship between the loss of RPE and choriocapillaris. In AMD eyes with drusen, a number of studies have reported that the locations where drusen form are associated with a loss of underlying choriocapillaris and choroidal vasculature.[2,5–7] This suggests that drusen are more likely to form in poorly or nonperfused regions of the choriocapillaris and choroid. Moreover, decreased perfusion of the choriocapillaris may precede any noticeable change in the RPE, and this perfusion alteration could be a cause of subretinal neovascularization in exudative AMD.[4] Similar findings of choriocapillaris degeneration are found in diabetes.[8–10] From these studies, it would follow that the ability to visualize and quantify changes in the choriocapillaris blood flow should prove useful for the early detection of perfusion abnormalities and their progression in normal aging and in different diseases. However, due to the pigmented nature of the RPE and the fenestrations in the choriocapillaris, it has been challenging to image the choriocapillaris in vivo.[11,12]

Fluorescein angiography (FA) is unable to visualize the choriocapillaris due to absorption of the excitation wavelength by the RPE and the diffuse leakage of fluorescein from the fenestrated choriocapillaris.[13] While indocyanine green angiography (ICGA) can visualize the larger choroidal vessels in vivo, it is unable to provide detailed visualization of the choriocapillaris because of the much higher background levels of

fluorescence arising from the larger underlying choroidal vessels early in the angiogram and the lack of structural resolution at the level of the fenestrated capillaries late in the angiogram due to extravascular accumulation of ICG.[14] Hence, most studies of the choriocapillaris have been limited to histology or indirect observations.[2–4,12]

Optical coherence tomography angiography (OCTA) provides the first opportunity to safely and routinely image the choriocapillaris in vivo.[15–17] OCTA identifies blood flow in vivo by utilizing the changes in both intensity and phase information from the motion of red blood cells identified from repeated OCT scans at the same position.[18–20] Several studies have used either spectral-domain (SD) or swept-source (SS) OCTA to image the choriocapillaris.[15–17] These studies focused on the morphologic or qualitative imaging of choriocapillaris. Recently, Spaide[21] used SD-OCTA to quantify flow voids (FVs) within the choriocapillaris in subjects at different ages and with different underlying diseases. He used a linear log–log plot with a goodness-of-fit method and showed that the data followed a power law distribution based on age and the diagnoses of hypertension, late AMD, and reticular pseudodrusen (RPD). Nesper et al.[22] also used SD-OCTA to image eyes with RPD and found that these eyes had significantly larger areas of choriocapillaris nonperfusion compared with eyes without RPD and eyes with drusen. Both studies showed the ability of SD-OCTA to detect changes in eyes with underlying disease.

While SD-OCTA might prove useful in eyes with ocular pathology that has little effect on the overall RPE morphology, SD-OCTA will have difficulty imaging the choriocapillaris when the RPE is elevated.[22–26] This is due to the instrument's wavelength of 840 nm, which is highly scattered by the RPE, thus limiting light penetration into choroid and signal reflections from the sub-RPE layers. To mitigate this issue, a longer wavelength is preferred. Previously, Choi et al.[17] noninvasively visualized the choriocapillaris lobules by using an ultrahigh-speed (400 kHz) SS-OCTA instrument operating at a wavelength of 1050 nm. Their images compared favorably to histopathologic specimens. By using the same experimental system, Choi et al.[27] also visualized choriocapillaris abnormalities in subjects with GA secondary to AMD. More recently, Gorczynska et al.[28] demonstrated histology-like resolution of the choriocapillaris lobules and deeper choroidal vessels using a SS-OCTA instrument scanning at an unprecedented acquisition speed of 1.7 MHz. The choriocapillaris meshwork of these healthy volunteers resembled histologic images. While ultrahigh-speed SS-OCT systems have demonstrated great potential for imaging the choriocapillaris in vivo, they are experimental laboratory based systems.

In this study, we used a commercially available SS-OCTA instrument (PLEX Elite 9000; Carl Zeiss Meditec, Inc., Dublin, CA, USA) to investigate the ability of a longer wavelength system to image the choriocapillaris in vivo. Using an earlier SS-OCTA prototype, we previously showed the superiority of SS-OCTA compared with SD-OCTA for the visualization of choroidal neovascularization.[23,24] In the current study, we used an improved SS-OCTA system (PLEX Elite 9000, Carl Zeiss Meditec, Inc.) to image the choriocapillaris, and we also developed a strategy to compensate for most of the signal attenuation that may arise from the overlying RPE/BM complex. This study also uses a strategy for quantifying areas of decreased choriocapillaris perfusion that should prove useful for characterizing pathologic changes and monitoring disease progression. Finally, repeatability of the method was performed on both normal and drusen eyes.

Methods

Subjects

All subjects were enrolled at the Bascom Palmer Eye Institute in a prospective OCT imaging study. The Institutional Review Board of the University of Miami Miller School of Medicine approved the study, and an informed consent to participate in the prospective OCT study was obtained from all subjects. The study was performed in accordance with the tenets of the Declaration of Helsinki and compliant with the Health Insurance Portability and Accountability Act of 1996.

Image Acquisition and Scanning Protocols

The instrument used in this study was a SS-OCTA system (PLEX Elite 9000, Carl Zeiss Meditec, Inc.), running at 100 kHz, that is 100,000 A-scans per second. This instrument is characterized by a central wavelength of 1060 nm, a bandwidth of 100 nm, an A-scan depth of 3.0 mm in tissue, a full-width at half maximal (FWHM) axial resolution of ~5 μm in tissue, and a lateral resolution at the retinal surface estimated at ~12 μm. FastTrac motion correction software (Carl Zeiss Meditec, Inc.) was used while the images were acquired. A scan with a nominal field of view (FoV) of 3 × 3 mm (equivalent to an angular view of 10.47 × 10.47 degrees measured in air at the pupil plane) centered on fovea was acquired on all the subjects. The scan contained 300 A-lines × 300 locations with four repeated scans in each fixed location. The complex optical microangiography (OMAG^{c}) algorithm was used to obtain OCTA images. This algorithm utilizes the variations in both the intensity and phase information between sequential B-scans at the same location to generate the motion signal, which indicates blood flow.[18] A validated semiautomated segmentation algorithm was applied to identify relevant retinal layers,[29] and manual corrections were carried out as necessary to ensure accurate segmentation. In particular, we evaluated en face angiograms of the choriocapillaris slab, which was defined by a layer starting at the outer boundary of BM and ending at approximately 20 μm beneath BM. A maximum projection was applied on the segmented volumes to generate the en face angiograms. Images were excluded from the study if significant media opacity was present, if signal strength was less than seven as defined by manufacturer, which prevented high-quality imaging, if there was severe motion artifact, or if any other macular pathology was present except drusen.

OCTA scans with nominal 3 × 3 mm pattern were also acquired approximately 9 mm inferior-nasal, and 12 mm temporal to the central fovea to facilitate qualitative comparison with characteristic scanning electron microscopic images as a function of distance from the fovea.

Method for Measuring Choriocapillaris Flow Voids

A novel approach was developed to compensate for choriocapillaris signal attenuation resulting from structural changes in the RPE/BM complex. To achieve this compensation, we used the structural information from the same slab used to image the blood flow in the choriocapillaris. The algorithm consisted of preprocessing and signal compensation. For the preprocessing, the choriocapillaris layer was first segmented from the structural OCT and the associated flow slab was then identified from the angiogram. A maximum projection was applied to both the three-dimensional structural and flow slabs to generate the en face choriocapillaris images. For eyes with drusen, another layer from the RPE to BM was also segmented from the structural data set to isolate a drusen map. Since the

Investigative Ophthalmology & Visual Science

incident light becomes more attenuated when passing through the RPE/BM complex due to its highly scattering property, a shadow is cast beneath the drusen. The attenuated light is then backscattered by the static tissue and moving blood cells of the choriocapillaris, and this signal is further attenuated by the RPE/BM complex before being detected by the OCT system. The shadowing effect under drusen was seen as a decreased signal on both structural and flow en face choriocapillaris images compared with nondrusen regions. Therefore, it is straightforward to consider using structural signal from the choriocapillaris to compensate for the attenuated flow signal in the choriocapillaris image. To eliminate the influence of the shadowing effect on the quantitation of FVs, we developed a strategy to compensate for the signal attenuation by utilizing the en face structural choriocapillaris image.

To simplify the procedure in our study, we used the two dimensional en face choriocapillaris structural image instead of the three-dimensional data. An inverse transformation was first applied to the en face structural choriocapillaris image to enhance the attenuated signal under drusen, where a Gaussian smoothing filter (3 × 3 pixel kernel) was used to minimize speckle noise. Then, a simple multiplication between the en face choriocapillaris flow image and the smoothed, inverted choriocapillaris structural image was performed, as shown in the following equation:

$$F_{Compensated} = F_{CC} \times (1 - Norm(S_{CC})) \quad (1)$$

Where $Norm()$ represents the normalization operation of the image; S_{CC} is the structural choriocapillaris image; F_{CC} is the choriocapillaris angiogram. Finally, the compensated choriocapillaris flow image was obtained. To provide a fair comparison between the original and compensated choriocapillaris results, projection artifacts from the retinal layers were eliminated by using our previous method[30] and drusen were highlighted from the drusen map and overlaid on the artifact-free images. The shadowing effect under drusen was compensated while the signal in the normal region remained the same, indicating the usefulness of our method (see Results).

FVs were defined as a percentage between the region that is absent from flow and the total scanned region, as follows:

$$FV = \frac{Area_{Flowvoid}}{Area_{whole}} \times 100\% \quad (2)$$

Where $Area_{Flowvoid}$ is the area with absence of flow; $Area_{whole}$ is the area of the entire image, which measured 3 × 3 mm. To isolate the areas with absence of flow from choriocapillaris, a threshold determined by the standard deviation of the artifact-free en face angiogram from a normal database was applied to each choriocapillaris image:

$$Area_{Flowvoid} = \sum_{i,j=1}^{i,j=300} (I_{mean} - I(i,j)) > n \text{ SD} \quad (3)$$

Where I_{mean} indicates the mean value of the entire image; $I(i,j)$ indicates the intensity value of individual pixel; i,j represents the row and column indices of the image with a maximum value of 300 × 300 in the nominal 3 × 3 mm images; n represents a positive number; SD is the standard deviation (SD) of the choriocapillaris images obtained from normal data sets (see Results). Since relative large retinal vessels would also cast shadows on the CC map due to blood absorption, we removed the vessel shadow regions by using retinal vessel map as the reference. After doing so, the FVs quantification will not be affected by the retinal shadows.

Repeatability Study

To validate our method and test the repeatability of FV quantitation, three repeated scans were collected on one of the eyes of each subject. For each imaged eye, two coefficient of variations (CVs) were calculated from three scans to evaluate the intravisit repeatability for FV measurements based on the original and compensated choriocapillaris angiograms.

Results

Twenty normal subjects and 12 patients with drusen were enrolled at the Bascom Palmer Eye Institute between February 2016 and May 2017. The normal subjects had a mean age of 52 ± 18.2 years old (range, 26–84) and the subjects with drusen had a mean age of 77 ± 5.3 years old (range, 69–86). All subjects were reviewed to confirm as normal control or drusen eyes. The right eye of each subject was chosen for this study, unless image quality was unacceptable. Each selected eye underwent three repeated scans. All the scans were included in the analyses.

Choriocapillaris Imaging With SS-OCTA

The en face angiogram under the central fovea showed a dense, lobular appearance (Fig. 1A). The lobules were small, densely packed, and demonstrated a uniform signal on the SS-OCTA images. However, the lobular pattern of the choriocapillaris became less dense toward the periphery (Figs. 1B, 1C) where larger, radially elongated lobules were observed. In addition, the diameter of the capillaries increased toward the periphery with corresponding wider and more elongated intercapillary spaces. The intercapillary spaces identified as FVs in normal subjects were clearly observed in SS-OCTA images, particularly in inferior-nasal and temporal regions. By comparing the SS-OCTA images with published anatomical images of a healthy eye (Figs. 1D, 1E, 1F),[31] we concluded that our SS-OCTA system using a 1060-nm central wavelength was able to image the choriocapillaris, which allowed us to proceed with quantitation of FVs in normal and diseased subjects. The imaging size of the OCTA images in Figures 1A, 1B, and 1C was 3 × 3 mm (10.47 × 10.47 degrees).

Measuring Choriocapillaris FVs

Figure 2 is a drusen case chosen to illustrate the strategy used to compensate for the signal attenuation resulting from changes in the RPE/BM complex. The choriocapillaris layer was first segmented from the structural OCT (Fig. 2A, yellow dash lines), and the associated flow slab was then identified from the OCTA angiogram (Fig. 2D). A maximum signal projection was used to generate the three-dimensional structural and flow en face choriocapillaris images from the same slabs (Figs. 2B, 2E), respectively. In addition, another slab extending from the RPE (blue dash line) to BM (the top yellow dash line) was segmented from the structural data set to isolate the drusen map (Fig. 2J). The shadowing effect shown as a decreased signal under drusen was observed in both the structural and flow en face choriocapillaris images (Figs. 2B, 2E). As described in the Methods section, utilizing the inverted en face structural slab (Fig. 2C) in Equation 1, the shadowing effect was compensated on the choriocapillaris flow image as shown in Figure 2F. To better visualize and compare the original and compensated choriocapillaris flow images, we removed the retinal projection artifacts arising from the retinal circulation (Fig. 2G) that were projected onto the choriocapillaris flow images as previously described (Figs. 2H, 2I).[30] The drusen profiles from the drusen map were then overlaid on the

Investigative Ophthalmology & Visual Science

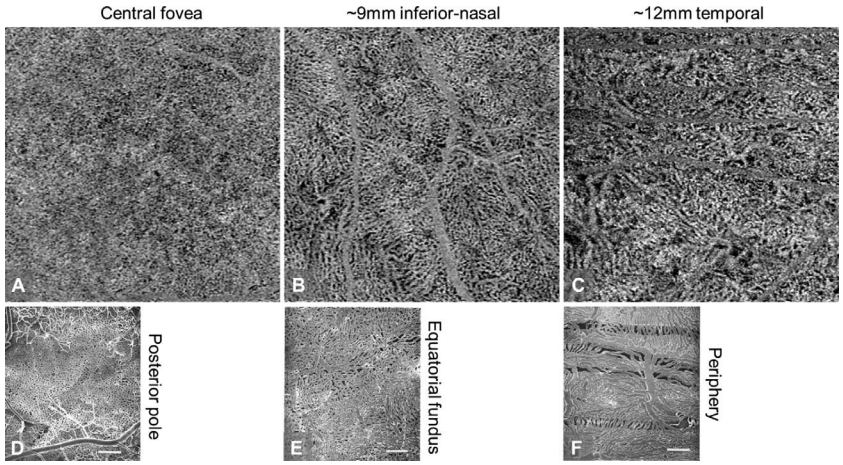

Figure 1. SS-OCTA images and scanning electron microscopic (SEM) images of choriocapillaris. **A**, **B**, and **C** are the typical OCTA images acquired at the locations of central fovea, approximately 9 mm inferior-nasal, and 12 mm temporal to the central fovea, respectively; **D**, **E**, and **F** are the SEM images of a healthy eye at the locations of posterior pole, equatorial fundus and periphery, respectively,[30] which approximately correspond to the fundus locations as shown in **A**, **B**, and **C**. The imaging size of **A**, **B**, and **C** is 3 × 3 mm (10.47 × 10.47 degrees). The *scale bar* in **D**, **E**, and **F** is 250 μm.

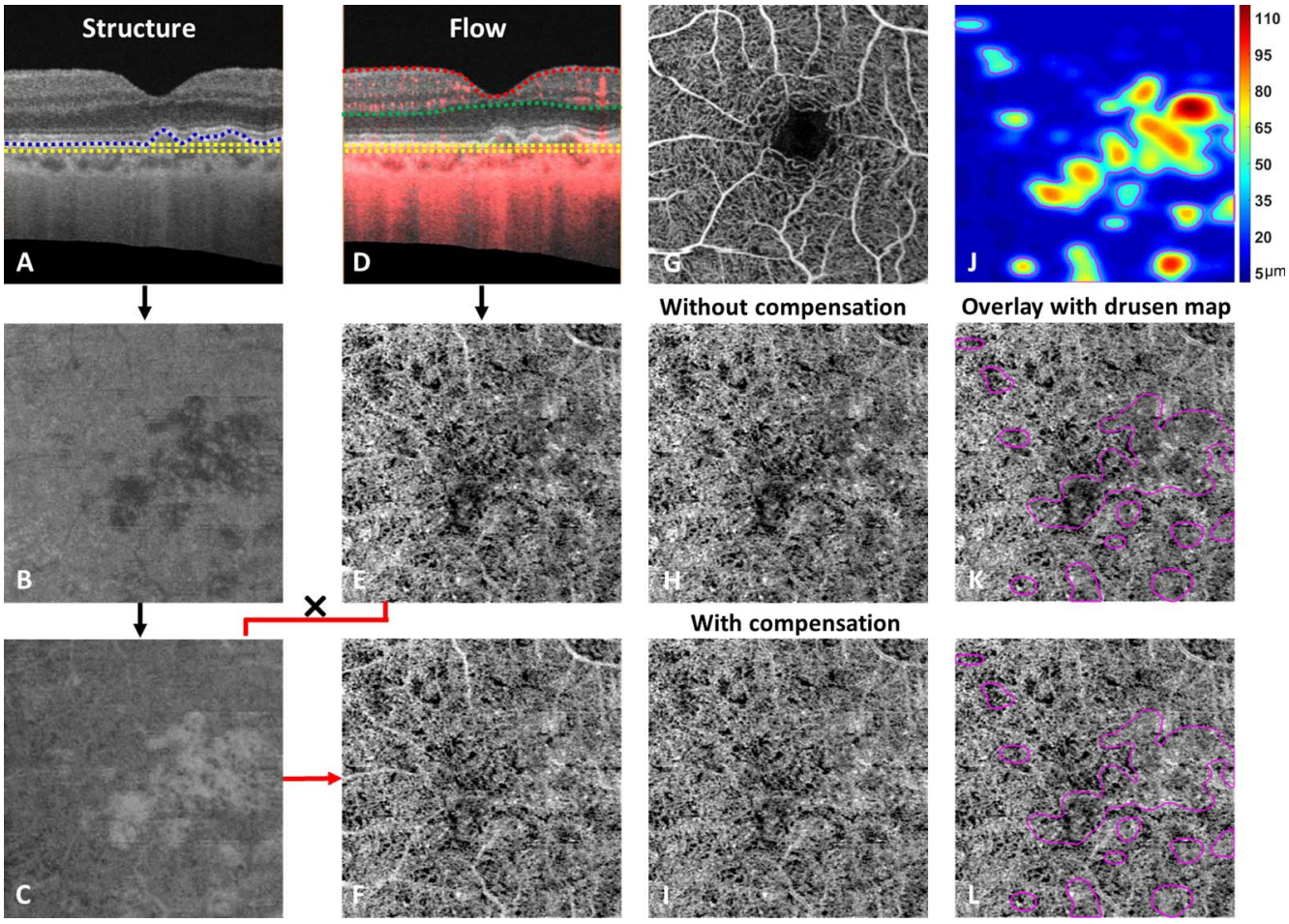

Figure 2. Signal compensation method to enhance the attenuated signal under drusen. (**A**) Cross-sectional structural OCT image with segmentation lines; (**B**) en face structural CC image; (**C**) inverted and smoothed structural CC image; (**D**) cross-sectional structural combined flow OCT image with segmentation lines; (**E**) en face flow CC image; (**F**) compensated flow CC image; (**G**) en face retinal OCTA image; (**H**) projection artifact-free original CC flow image; (**I**) projection artifact-free CC flow image with compensation; (**J**) drusen map, coded from cold *blue color* (no elevation) to hot *red color* (maximum elevation height of the RPE); (**K**) original CC flow image overlaid with drusen; and (**L**) compensated CC flow image overlaid with drusen. Drusen are outlined with *magenta color* in **J**, **K**, and **L**.

Investigative Ophthalmology & Visual Science

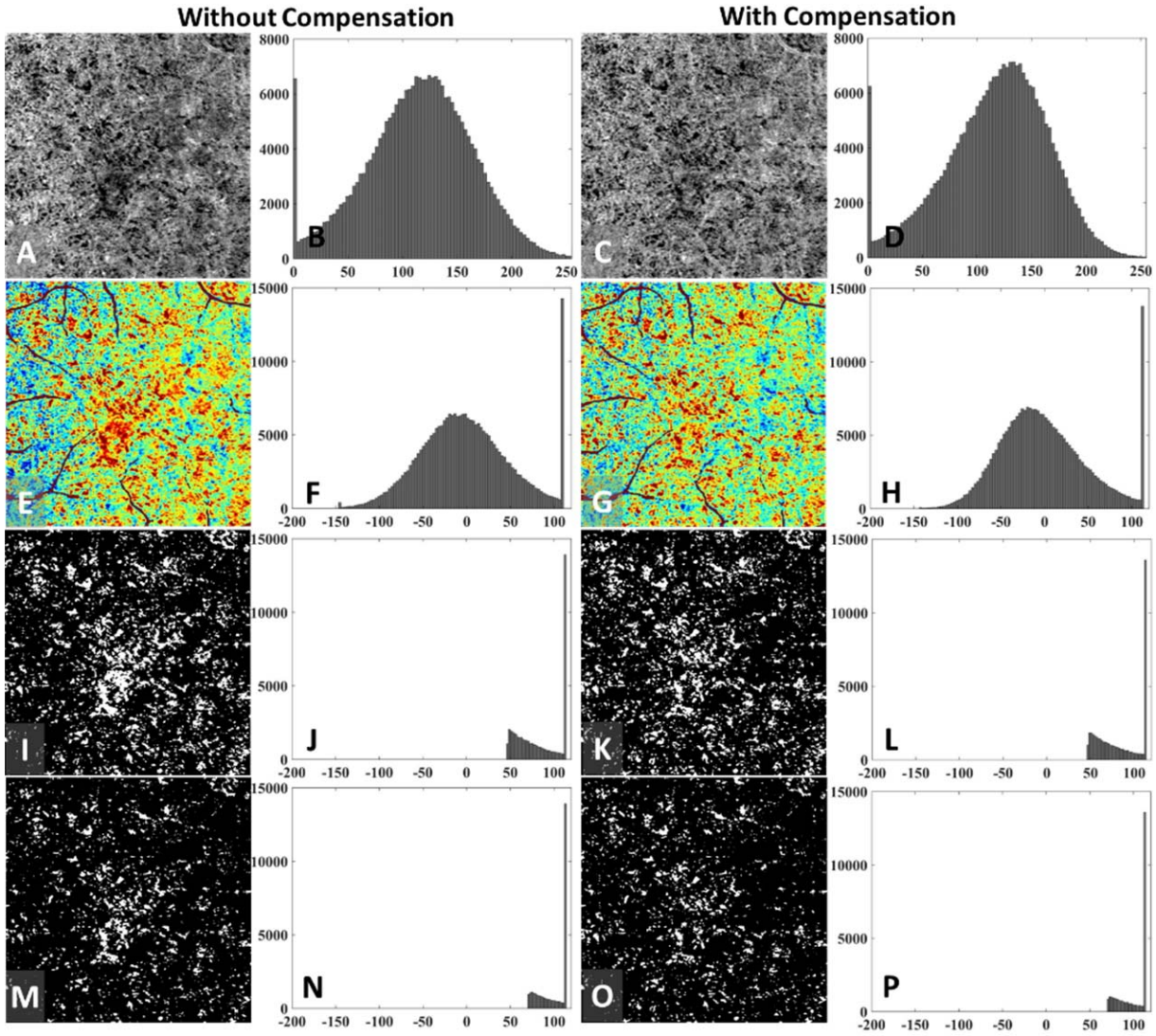

FIGURE 3. The processing steps to isolate the FVs from the choriocapillaris (CC) angiograms. (**A**) Original CC image without compensation; (**B**) histogram distribution of image A; (**C**) CC image with compensation; (**D**) histogram distribution of image C; (**E**, **G**) color-coded fluctuation maps of **A** and **C** from a low probability of a FV (*blue color*) to a high probability of a FV (*red color*), respectively; (**F**, **H**) histogram distribution of **E** and **G**; (**I**, **K**) FVs (*white*) isolated from fluctuation maps (**E**, **G**), respectively, by using 1 SD of the normal database. (**J**, **L**) Histogram distribution of image **I** and **K**. (**M**, **O**) FVs isolated from fluctuation maps (**E**, **G**), respectively, by using 1.5 SD of normal database. (**N**, **P**) Histogram distribution of image **M** and **O**.

artifact-free images (Figs. 2K, 2L). Visually, the shadowing effect from the drusen was decreased in some areas while the decreased signal from the regions without drusen remained the same, indicating the potential usefulness of our method.

FVs were identified using a thresholding method based of artifact-free en face angiograms obtained from normal controls (Equation 3). Instead of using a single SD from an individual image, we used a mean SD from a normal database including 20 subjects with ages from 20 to 39 years old. The mean SD of the normal database was approximately 47 in gray level with a dynamic range of an image from 0 to 255. The reason we used a younger age group is that the young subjects have a greater likelihood of having a normal choriocapillaris pattern, thus minimizing the effect of age. However, the optimal value of the multiplier n to be used in the threshold (Equation 3) for the segmentation of FVs is an open question. Figure 3 provides the detailed procedure for the selection of n. Figures 3A and 3C show the results from the choriocapillaris image without and with structural compensation, respectively. Histograms of the angiogram without (Fig. 3B) and with (Fig. 3D) compensation were first plotted to illustrate the signal distribution within the choriocapillaris, which appear as skewed Gaussian distributions. Usually, a simple way to select a threshold is to remove the signal below a predefined value based on the histogram of images. However, no predefined value had been established previously. To find a reasonable threshold, the fluctuation signals were calculated based on Equation 3 in the Methods section (i.e., $I_{mean} - I(i,j)$) and represented in Figures 3E and 3G. The corresponding histograms (Figs. 3F, 3H) were used to illustrate the variation of choriocapillaris signals, where the red color represents a positive fluctuation signal that has a higher possibility to be a FV and blue represents a small or negative value with a low possibility to be a FV. A threshold was then identified on the histogram of the fluctuation map, which was determined by the SD of normal database, to isolate FVs. Figures 3I to 3L and Figures 3M to 3P illustrate the results of segmented FVs with different thresholds of 1 SD and 1.5 SD, respectively. As expected, a larger threshold resulted in fewer

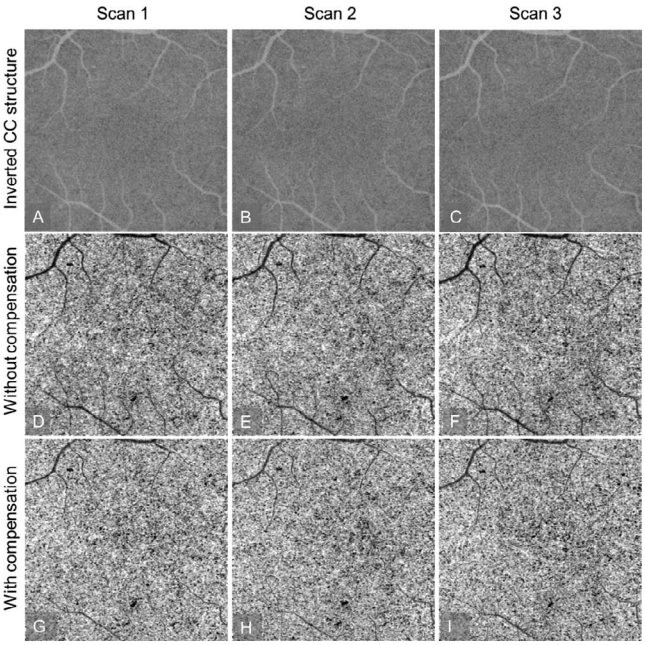

Figure 4. The en face choriocapillaris images from the central fovea of a 27-year-old normal subject with three repeated scans. **(A–C)** The inverted choriocapillaris structure image; **(D–F)** choriocapillaris angiograms without compensation; **(G–I)** choriocapillaris angiograms compensated by choriocapillaris structure information. The image size is 3 × 3 mm (10.47 × 10.47 degrees).

FVs and vice versa. Overall, the structurally compensated choriocapillaris angiogram had fewer FVs compared to the original choriocapillaris, no matter what threshold was used, indicating that the attenuated signal caused by drusen had been compensated by using the structural image.

Repeatability Study

Figure 4 shows an example of en face choriocapillaris images from the central fovea of a 27-year-old normal subject with three repeated scans. Excellent intravisit repeatability of the choriocapillaris patterns can be observed. Figures 4A to 4C are the inverted en face structural choriocapillaris images used for the signal compensation. Figures 4D to 4F are the original choriocapillaris images without compensation, and Figures 4G to 4I are the choriocapillaris images compensated with structural information. With compensation, a more uniform distribution of the choriocapillaris was observed in Figures 4G to 4I compared with a less uniform vascular pattern seen in the original choriocapillaris angiogram (Figs. 4D–F).

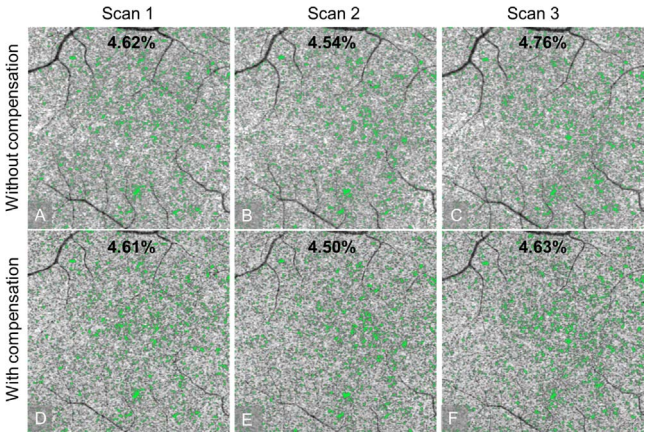

Figure 5. FV segmentation of three repeated scans judged by 1 SD of the normal database. **(A–C)** without compensation; **(D–F)** with compensation. The percentage of FVs (values shown in *top* of each image) was less after compensation. *Green color* represents the FVs.

In Figure 5, FVs, shown in green, were determined by using 1 SD as a threshold. The results showed slightly smaller FV values after structural compensation, with a mean value of 4.58% with compensation versus 4.64% without compensation. Excellent FV repeatability can be obtained with a CV of 2.4% without compensation and a CV of 1.5% with compensation.

Drusen cases were also analyzed and an example is shown in Figure 6. To illustrate the influence of drusen on the imaging of the choriocapillaris, drusen maps were segmented from RPE to BM and shown in Figures 6A to 6C. Signal reduction was observed under drusen on the choriocapillaris angiograms, which resulted in an increase in the number of FVs compared with the normal eye. This may be caused by the actual loss of choriocapillaris flow under drusen (Figs. 6D–F, red arrows) or the shadowing effect caused by drusen and an elevated RPE/BM complex (Figure 6D–F, yellow arrows). After compensating with structural information, we show that the shadowing effect on the choriocapillaris was diminished as demonstrated in the bottom two rows in Figure 6, while the areas consistent with decreased choriocapillaris flow are still present. The FV segmentations based on 1 SD thresholding are shown by the green color in Figure 6. A mean measurement of FVs was 18.06% in the original choriocapillaris angiograms, and after structural compensation, the mean FV measurement decreased to 15.93%. Excellent FVs repeatability was obtained with a CV of 3.2% without compensation and a smaller CV of 1.9% with compensation.

The intravisit repeatability for the FV measurements and the corresponding CVs for the choriocapillaris angiograms are shown in the Table. Three thresholds of 1, 1.25, and 1.5 SD

Table. Intravisit Repeatability of Choriocapillaris Flow Voids Measured in Normal and Drusen Eyes

	Threshold	Flow Voids (FV %) (1.0 SD)	Coefficient of Variation (CV %) (1.0 SD)	Flow Voids (FV %) (1.25 SD)	Coefficient of Variation (CV %) (1.25 SD)	Flow Voids (FV %) (1.5 SD)	Coefficient of Variation (CV %) (1.5 SD)
Normal (20)	Without compensation	10.56 ± 3.83	5.82 ± 4.35	7.25 ± 3.22	7.16 ± 5.36	4.92 ± 2.59	8.66 ± 6.36
Flow voids	With compensation	10.31 ± 3.66	5.35 ± 3.88	7.05 ± 3.02	6.43 ± 4.93	4.76 ± 2.40	7.77 ± 6.02
Drusen (10)	Without compensation	21.97 ± 3.91	5.87 ± 6.30	17.77 ± 3.87	7.53 ± 8.83	14.21 ± 3.72	9.51 ± 11.55
Flow voids	With compensation	19.83 ± 3.94	5.73 ± 6.53	15.84 ± 3.87	7.13 ± 8.61	12.54 ± 3.67	8.46 ± 10.86

Flow voids and CVs are presented as mean ± SD.

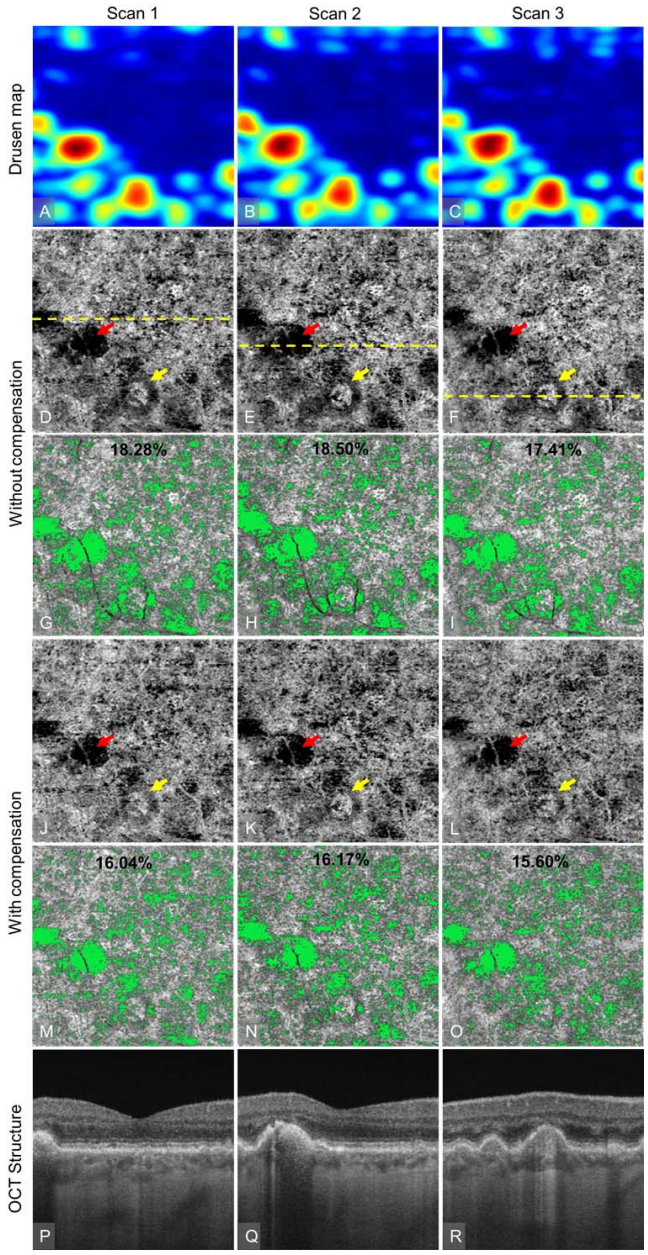

Figure 6. An example of three repeated en face choriocapillaris images from an eye with drusen. The *top row* (**A–C**) shows drusen maps from each scan, coded from *blue* (no elevation) to *red* (maximum elevation). The *middle* two rows show the choriocapillaris angiograms (**D–F**) and segmentation of the FVs (**G–I**). The next two rows show the choriocapillaris angiograms compensated by using structural information (**J–L**) and the corresponding images showing FV segmentation (**M–O**). The *bottom* row (**P–R**) shows the OCT structural images located in the *yellow lines* in **D**, **E**, and **F**. *Red arrows* indicate areas with decreased choriocapillaris flow under drusen. *Yellow arrows* indicate the shadow effect under drusen that was compensated by structural information.

were computed of each case to test the intravisit repeatability. In normal and drusen cases, the FV measurements with 1.0 SD as a threshold showed the best repeatability, followed by 1.25 and 1.5 SD. It was apparent that higher thresholds resulted in fewer choriocapillaris FVs and lower repeatability. In general, the percentage of FVs was less after signal compensation in both normal and drusen case while the repeatability was improved after compensation.

Discussion

SS-OCTA is able to image the choriocapillaris in vivo and areas with decreased perfusion can be quantified with high repeatability in both normal eyes and eyes with drusen. We used a method to compensate for the signal loss caused by the RPE/BM complex, which is an important achievement when quantifying the appearance and progression of FVs in eyes with drusen due to the shadowing effect from the elevated RPE. Several studies have reported the quantitation of FVs or areas of decreased choriocapillaris perfusion based on OCTA imaging, but none of them did studies to test the repeatability of their methods, and the threshold for the segmentation of the FVs was subjectively selected based on each individual image.[21,22] Nesper et al.[22] presented RPD cases with significantly larger areas of choriocapillaris nonperfusion compared with eyes with drusen and no RPD, but they excluded the RPD region when they quantified the area of choriocapillaris nonperfusion. Another possible limitation of these studies was that they utilized a SD-OCTA system that employed a shorter wavelength of 840 nm, which limits the light penetration under the RPE.

In our report, we conducted a repeatability study using SS-OCTA that allowed for deeper light penetration into the choroid.[23,24] In addition, we proposed a method of using the structural information to compensate for the flow signal attenuation caused by the RPE/BM complex in order to recover the attenuated signal and improve the choriocapillaris image. If not accounted for, this signal attenuation could introduce a shadowing effect on the choriocapillaris flow image, particularly in cases where the RPE/BM complex is elevated, such as under drusen. Moreover, an SD based thresholding method was used to isolate FVs in the choriocapillaris angiograms. Instead of using individual SD for each image, we used an average SD from a normal database consisting of 20 subjects with an age group from 20 to 39 years old. This threshold eliminated the compounding factor of age on choriocapillaris angiograms. While the optimal threshold value needed to deliver an accurate segmentation of FVs is not yet determined, the observed trend was that the percentage of FVs was similar when using various thresholds that were determined by the SD. According to our findings, 1 SD showed good results in measuring FVs both in normal and druse cases.

One limitation of this study is that we involved only healthy subjects and subjects with drusen to test the repeatability of FV measurements in the choriocapillaris. Since this was the first study testing repeatability of choriocapillaris FV quantitation, we started with normal subjects and patients with drusen to make sure that the measurements could be achieved with minimal pathology. The next challenge will be to image eyes with more severe disease involving larger elevations of the RPE and macular fluid, which may cause greater attenuation of the signal and decrease the repeatability of the images. In addition, the proposed algorithm may not be effective in cases where the reflectivity of the RPE/Bruchs complex is highly variable. Thus, further investigations are needed in eyes with larger pigment epithelial detachments, macular edema, macular neovascularization, and also in cases where the RPE reflectivity is highly variable. While we are unable to determine the absolute accuracy of our method at this time due to the lack of an established gold standard for flow-voids segmentation in vivo, our proposed flow-voids segmentation method provided visually good results and produced excellent repeatability when using a threshold of 1.0 SD. Clearly, the quantitative accuracy of this method warrants a further investigation.

Investigative Ophthalmology & Visual Science

This study only focused on the repeatability of the FVs identification on normal and drusen eyes, thus, it would be inappropriate to make comparisons between the healthy and drusen groups in the design. Further studies are needed to investigate the difference between normal and diseased eyes.

In conclusion, we have shown that SS-OCTA has the ability to detect the choriocapillaris and FVs can be quantified. A novel method was proposed to compensate for the signal attenuation in choriocapillaris angiograms caused by RPE and BM complex by using the associated structural images. Measurements of FVs were performed on both the original and compensated choriocapillaris angiograms resulting in excellent repeatability. The ability of SS-OCTA to quantify the choriocapillaris should prove useful in understanding disease pathogenesis, improving early diagnoses, monitoring disease progression, and following response to treatment.

Acknowledgments

Supported by grants from Carl Zeiss Meditec, Inc. (Dublin, CA, USA), the National Eye Institute (R01EY024158), an unrestricted grant from the Research to Prevent Blindness, Inc. (New York, NY, USA), and the National Eye Institute Center Core Grant (P30EY014801) to the Department of Ophthalmology, University of Miami Miller School of Medicine. The funding organization had no role in the design or conduct of this research.

Disclosure: **Q. Zhang**, None; **F. Zheng**, None; **E.H. Motulsky**, None; **G. Gregori**, Carl Zeiss Meditec, Inc. (F), P; **Z. Chu**, None; **C.-L. Chen**, None; **C. Li**, None; **L. de Sisternes**, Carl Zeiss Meditec, Inc. (E); **M. Durbin**, Carl Zeiss Meditec, Inc. (E); **P.J. Rosenfeld**, Acucela (C), Appellis (F, I), Biotech (C), Boehringer-Ingelheim (C), Carl Zeiss Meditec, Inc. (C, F), Cell Cure Neurosciences (C), Chengdu Kanghong (C), Digisight (I), Genentech (C, F), Healios K.K. (C), F. Hoffmann-La Roche Ltd (C), MacRegen, Inc. (C), Ocudyne (C, I), Ocunexus Therapeutics (C), Tyrogenex, (C, F), Unity Biotechnology (C); **R.K. Wang**, Carl Zeiss Meditec, Inc. (C, F), Insight Photonic Solutions (C), P

References

1. Wybar KC. A study of the choroidal circulation of the eye in man. *J Anat*. 1954;88:94–98.
2. Lutty G, Grunwald J, Majji AB, Uyama M, Yoneya S. Changes in choriocapillaris and retinal pigment epithelium in age-related macular degeneration. *Mol Vis*. 1999;5:35.
3. Sarks JP, Sarks SH, Killingsworth MC. Evolution of geographic atrophy of the retinal-pigment epithelium. *Eye*. 1988;2:552–577.
4. McLeod DS, Grebe R, Bhutto I, et al. Relationship between RPE and choriocapillaris in age-related macular degeneration. *Invest Ophthalmol Vis Sci*. 2009;50:4982–4991.
5. Friedman E, Smith TR, Kuwabara T. Senile choroidal vascular patterns and drusen. *Arch Ophthalmol*. 1963;69:220–230.
6. Sarks SH, Arnold JJ, Killingsworth MC, Sarks JP. Early drusen formation in the normal and aging eye and their relation to age related maculopathy: a clinicopathological study. *Br J Ophthalmol*. 1999;83:358–368.
7. Lengyel I, Tufail A, Hosaini HA, et al. Association of drusen deposition with choroidal intercapillary pillars in the aging human eye. *Invest Ophthalmol Vis Sci*. 2004;45:2886–2892.
8. Cao J, McLeod S, Merges CA, Lutty GA. Choriocapillaris degeneration and related pathologic changes in human diabetic eyes. *Arch Ophthalmol*. 1998;116:589–597.
9. Fryczkowski AW, Hodes BL, Walker J. Diabetic choroidal and iris vasculature scanning electron microscopy findings. *Int Ophthalmol*. 1989;13:269–279.
10. Gerl VB, Bohl J, Pitz S, et al. Extensive deposits of complement C3d and C5b-9 in the choriocapillaris of eyes of patients with diabetic retinopathy. *Invest Ophthalmol Vis Sci*. 2002;43:1104–1108.
11. Bill A, Sperber G, Ujiie K. Physiology of the choroidal bed. *Int Ophthalmol*. 1983;6:101–107.
12. Flower RW, Fryczkowski AW, McLeod DS. Variability in choriocapillaris blood flow distribution. *Invest Ophthalmol Vis Sci*. 1995;36:1247–1258.
13. Cohen SM, Shen JH, Smiddy WE. Laser energy and dye fluorescence transmission through blood in vitro. *Am J Ophthalmol*. 1995;119:452–457.
14. Von Sallmann L. The structure of the eye. *Arch Ophthalmol*. 1961;66:920–921.
15. Braaf B, Vienola KV, Sheehy CK, et al. Real time eye motion correction in phase-resolved OCT angiography with tracking SLO. *Biomed Opt Express*. 2013;4:51–65.
16. Kurokawa K, Sasaki K, Makita S, Hong Y-J, Yasuno Y. Three dimensional retinal and choroidal capillary imaging by power Doppler optical coherence angiography with adaptive optics. *Opt Express*. 2012;20:22796–22812.
17. Choi W, Mohler KJ, Potsaid B, et al. Choriocapillaris and choroidal microvasculature imaging with ultrahigh speed OCT angiography. *PLoS One*. 2013;8:e81499.
18. Wang RK, An L, Francis P, Wilson DJ. Depth-resolved imaging of capillary networks in retina and choroid using ultrahigh sensitive optical microangiography. *Opt Lett*. 2010;35:1467–1469.
19. An L, Subhush HM, Wilson DJ, Wang RK. High-resolution wide-field imaging of retinal and choroidal blood perfusion with optical microangiography. *J Biomed Opt*. 2010;15:026011.
20. Wang RK. Optical microangiography: a label free 3D imaging technology to visualize and quantify blood circulations within tissue beds in vivo. *IEEE J Sel Top Quantum Electron*. 2010;16:545–554.
21. Spaide RF. Choriocapillaris flow features follow a power law distribution: implications for characterization and mechanisms of disease progression. *Am J Ophthalmol*. 2016;170:58–67.
22. Nesper PL, Soetikno BT, Fawzi AA. Choriocapillaris nonperfusion is associated with poor visual acuity in eyes with reticular pseudodrusen. *Am J Ophthalmol*. 2017;174:42–55.
23. Zhang Q, Chen CL, Chu Z, et al. Automated quantitation of choroidal neovascularization: a comparison study between spectral-domain and swept-source OCT angiograms. *Invest Ophthalmol Vis Sci*. 2017;58:1506–1513.
24. Miller AR, Roisman L, Zhang Q, et al. Comparison between spectral-domain and swept-source optical coherence tomography angiographic imaging of choroidal neovascularization. *Invest Ophthalmol Vis Sci*. 2017;58:1499–1505.
25. Copete S, Flores-Moreno I, Montero JA, Duker JS, Ruiz-Moreno JM. Direct comparison of spectral-domain and swept-source OCT in the measurement of choroidal thickness in normal eyes. *Br J Ophthalmol*. 2014;98:334–338.
26. Lim LS, Cheung G, Lee SY. Comparison of spectral domain and swept-source optical coherence tomography in pathological myopia. *Eye*. 2014;28:488–491.
27. Choi W, Moult EM, Waheed NK, et al. Ultrahigh-speed, swept-source optical coherence tomography angiography in nonexudative age-related macular degeneration with geographic atrophy. *Ophthalmology*. 2015;122:2532–2544.
28. Gorczynska I, Migacz JV, Jonnal R, et al. Imaging of the human choroid with a 1.7 MHz A-scan rate FDML swept source OCT system. 2017. Proc. SPIE 10045, Ophthalmic Technologies XXVII, 1004510.

29. Yin X, Chao JR, Wang RK. User-guided segmentation for volumetric retinal optical coherence tomography images. *J Biomed Opt*. 2014;19:086020.
30. Zhang A, Zhang Q, Wang RK. Minimizing projection artifacts for accurate presentation of choroidal neovascularization in OCT micro-angiography. *Biomed Optics Express*. 2015;6: 4130–4143.
31. Olver JM. Functional anatomy of the choroidal circulation: methyl methacrylate casting of human choroid. *Eye*. 1990;4: 262–272.

Investigative Ophthalmology & Visual Science